DENTAL MATERIALS 35 (2019) e140–e152

Available online at www.sciencedirect.com

ScienceDirect

journal homepage: www.intl.elsevierhealth.com/journals/dema

Detection threshold of non-contacting laser profilometry and influence of thermal variation on characterisation of early surface form and textural changes in natural human enamel

Petros Mylonas[a,*], *Thomas Bull*[b], *Rebecca Moazzez*[a], *Andrew Joiner*[c], *David Bartlett*[a]

[a] *Centre for Oral, Clinical and Translational Sciences, King's College London Faculty of Dentistry, Oral & Craniofacial Sciences, UK*

[b] *Mechatronics Research Group, Engineering and the Environment, University of Southampton, UK*

[c] *Unilever Oral Care, Bebington, Wirral, UK*

ARTICLE INFO

Article history:
Received 22 November 2018
Received in revised form
14 March 2019
Accepted 1 April 2019

Keywords:
Freeform surface characterisation
Surface profilometry
Surface roughness
Optical coherence tomography
Dental erosion

ABSTRACT

Objectives. To determine the detection threshold of non-contacting laser profilometry (NCLP) measuring surface form and surface roughness change in natural human enamel *in vitro*, characterise how ambient scanning thermal variation affects NCLP measurement, and calculate bulk enamel loss in natural human enamel.

Methods. NCLP repeatability and reproducibility accuracy was determined by consecutively scanning natural human enamel samples with/without sample repositioning. Ambient thermal variation and NCLP sensor displacement over short (30 s), medium (20 min), and long (2 h) scanning periods were evaluated for their standard deviation. Natural human enamel specimens (n = 12) were eroded using citric acid (0.3% w/w pH3.2) for 5, 10, and 15 min and characterised using surface profilometry, tandem scanning confocal microscopy (TSM), and optical coherence tomography (OCT).

Results. Repeatability and reproducibility error of NCLP for surface form was 0.28 μm and 0.43 μm, and for surface roughness 0.07 μm and 0.08 μm. Ambient thermal variation resulted in NCLP sensor displacement of 0.56 μm and 1.05 μm over medium and long scanning periods. Wear scar depth (μm) was calculated between 0.72–1.61 at 5 min, 1.72–3.06 at 10 min, and 3.40–7.06 at 15 min. Mean (SD) surface roughness (μm) was 1.13 (0.13), 1.52 (0.23), 1.44 (0.19), and 1.43 (0.21) at baseline, 5, 10, and 15 min. Qualitative image analysis indicated erosive change at the surface level, progressing after increasing erosion time.

Significance. Minimum detectable limits for NCLP measuring surface form and surface roughness changes were characterised. Ambient thermal variation, subsequent sensor displacement, and its impact on NCLP performance were characterised. Dental erosion lesions in natural human enamel could be characterised using surface profilometry, surface roughness, OCT, and TSM. Step height formation could be calculated within NCLP and temperature operating limits using profile superimposition and profile subtraction techniques.

* *Corresponding author at*: Centre for Oral, Clinical and Translational Sciences, King's College London Faculty of Dentistry, Oral & Craniofacial Sciences, Room 36, Floor 17, Tower Wing, Guy's Hospital, London SE1 9RT, UK.
E-mail address: petros.mylonas@kcl.ac.uk (P. Mylonas).

https://doi.org/10.1016/j.dental.2019.04.003

Natural enamel samples can now be used in *in-vitro* studies to investigate the formation and development of early acid erosive tooth wear, as well as the assessment of methods for enamel lesion remineralisation and repair.

1. Introduction

Non-contacting laser profilometry (NCLP) is considered the gold standard measurement technique for the detection and quantification of surface wear in dental tribology and dental erosion studies of acid-mediated attack on dental hard tissue samples [1–3]. NCLPs utilise a laser displacement probe and precision motion system to map the surface topography of an object as a three-dimensional point cloud. The point cloud data can subsequently be analysed and compared, using metrology or superimposition software, to extract, quantify and compare the surfaces [1,4].

Quantification of the effects of acid-mediated erosion on enamel surfaces using NCLP have previously focused on extensively eroded surfaces, where the extent of the wear is clinically visible and thus well within the detection threshold of current NCLPs [5].

In dental erosion studies, the detection threshold of NCLPs is primarily determined by three factors: the size of the laser spot [6] determines lateral/spatial (XY) resolution, the optics of the displacement laser determines vertical/axial (Z) resolution, and lateral precision [4,6] of the motion system used which in-turn determines the repeatability of measurement.

Vertical resolution (Z height) is defined as the smallest measurable height difference between surface features, whilst lateral resolution (XY) is the smallest measurable distance between two surface features in the x–y plane [7]. Early erosive lesions have been previously characterised using changes in surface form [8] and surface roughness (amplitude parameter, Sa) [8,9].

Surface form and textural measurements can be affected by differences in both NCLP vertical and lateral resolution, and the step-over distance (sampling interval distance) of the motion system utilised [7,10]. Both the vertical and lateral resolution of the NCLP system are important for the detection threshold of early erosive lesions. Previously it has been shown that a lateral resolution <2.5 μm was sufficient to resolve surface textural features on the polished and natural enamel surface [11], and vertical resolution 10 nm to resolve small changes in surface form in polished enamel [8,12]; no study has yet to evaluate this in natural human enamel.

Surface form detection is dependent primarily on NCLP vertical resolution whilst surface roughness will be primarily affected by lateral resolution [6]. Surface form measurement comprises long wavelength features, compared to the short wavelength features for surface roughness.

NCLP detection threshold is therefore different depending on whether surface form or roughness is being measured; this has yet to be evaluated in natural human enamel. Evaluating both detection thresholds are important to ensure early erosion can be evaluated for changes in surface form and roughness.

However, other sources of error can affect the overall accuracy of NCLP measurement. Thermal variation during the period of the measurement is considered one of the largest sources of measurement error in surface metrology where the NCLP is required to detect submicron scale changes in surface texture or form [4,6,13,14]. Dimensional metrology studies in the manufacturing sector have demonstrated thermal induced measurement errors in X, Y, and Z axes using optical profiling to assess measurement accuracy [14]. To date, there have been no studies which have considered, measured, or determined the effects of thermal variation in dental surface metrology measurements with NCLPs.

Additional measurement error is also introduced depending on the enamel model utilised. Natural unpolished enamel is considered an organic freeform structure comprising a series of complex curved surfaces and randomly varying topographical features [15,16]. The topography of the enamel surface is highly variable due to the presence of: perikymata grooves which add wave-like concentric surface features, and focal holes and enamel caps which add additional peak and valley features [17], This results in an additional level of topography complexity increasing the difficulty of accurately measuring natural enamel surface features using NCLP; this is due to measurement errors inherent to scanning complex curved surfaces [6,10]. The nature of the surface topography also impacts on the formation and progression of acid-induced erosion which is non-uniform and heterogenous, and this increases the difficulty in characterising and measuring surface changes with NCLP [15,16,18]. As a result, polished enamel has been the most commonly used substrate to study the effects of acid-mediated erosion as the polishing process removes the aprismatic surface layer and produces a more topographically flat and uniform surface with near standardised surface characteristics [6,10].

The polishing process, however, affects the wear characteristics of enamel and its susceptibility to acid-induced erosion increases as the dentinal–enamel junction (DEJ) is reached [16]. The preservation of the outer amorphous surface layer of natural enamel may present a more representative substrate with which to study the *in vitro* effects of acid-mediated erosion and subsequent modifying factors or therapeutic agents [19,20].

Previous studies quantifying surface form change in natural or polished enamel samples have investigated the differences between before- and after-erosion datasets using either superimposition alignment with quantified Z-axis deviations [1,21], or by subtraction analysis involving the subtraction of before- and after- erosion datasets (with or without prior scan alignment) to produce a difference or residual

dataset from which form change is calculated [22,23]. These methods have either utilised NCLP with large spot size (15 μm) displacement sensors [1], handheld intraoral scanners [21], or white light interferometry [22], which are unable to detect very early surface form or roughness change *in vitro*. Additionally, these methods have yet to be investigated for suitability in measuring surface form and texture measurement using NCLP with very small spot size (2 μm) displacement sensor.

The aim of this study is therefore to investigate the minimum detectable threshold of surface profile and roughness changes in natural enamel and develop a relevant *in vitro* model to study the effects of early acid-induced erosion.

2. Materials and methods

2.1. Sample preparation

Extracted human permanent erupted-molar teeth free from clinical disease or prior restoration, were collected under ethical approval (REC: 12/LO/1836) and with patient informed consent. Twelve enamel sections were produced with approximately equal dimensions (5 mm × 5 mm × 3 mm), the buccal, palatal and/or lingual portions, were sectioned using a 300 μm diamond wafering blade, and fixed on 76 mm × 26 mm × 1 mm glass microscope slides (Marienfield GmbH & Co. KG, Germany) using epoxy resin (EverStick, Everbuild Products Ltd, UK) to produce microscope slides with 4 enamel specimens bonded to the surface; 2 buccal and 2 palatal or lingual sections from the same unpolished or natural surface from the tooth.

A bespoke positioning jig was manufactured to ensure repeatable placement of each microscope specimen slides onto the NCLP prior to scanning.

To ensure all samples were cleaned of all organic and inorganic surface contaminants, a minimally invasive cleaning process was utilised. This consisted of chemical-only cleaning technique involving 10-min immersion in 4.7% sodium hypochlorite, followed by 30-min ultrasonication in distilled water, air drying, then 2-min alcohol wipe using cotton buds. Samples were inspected under tandem scanning confocal microscopy (TSM) before and after cleaning to ensure cleanliness.

An overview of the study design can be seen in Fig. 1.

2.2. Investigation 1—detection threshold determination

An NCLP with a 655-nm confocal laser mounted on an automatic motion system (XYRIS 2000CL, Taicaan, Southampton, UK) was used throughout this study; the NCLP has a 2 μm lateral (XY) laser spot size, 10 nm axial (Z height) resolution and 0.6 mm Z-range. The repeatability study (instrument accuracy) was conducted by scanning one natural human enamel sample 10 times consecutively, according to good metrology scanning guidelines [13], without pick up and replacement, whilst for the reproducibility study (pick and replacement accuracy), the sample was scanned 10 times consecutively with the sample picked up and replaced on the scanning jig every 21 min; the time taken to complete one measurement. To ensure minimisation of thermal variation on scanning, the samples were allowed to thermally equilibrate for period of 10 min prior to initiating each scan.

To quantify NCLP precision (repeatability and reproducibility) in measuring surface form and surface roughness, the mean variability between the 10 measurements was calculated by firstly importing the data sets into surface metrology software (Boddies v1.92, Taicaan, Southampton, UK). Each surface scan consisted of a rectilinear grid (XY), with a height measurement (Z) taken at each intersection. Form and roughness data was extracted separately from the original raw profile data using a 0.8 μm Gaussian filter for form and roughness over a 10 μm sampling interval [4]. Differences between consecutive form and roughness data were then calculated by superimposing two measurement grids and subtracting one from the other. This difference was quantified by taking the absolute (modulus) of the difference at each measured point and calculating the arithmetic average (mean) of the absolute height differences between the measurements. In the case of perfectly matching data the measured points would all superimpose perfectly and there will be no difference. The detection threshold for both surface form and roughness was then calculated using a previously published method, using the equation mean + 3 SD; whereby mean and SD refer to the average and standard deviation in the arithmetic average (mean) of the absolute height differences between measurements [24].

2.3. Investigation 2—characterising the influence of thermal variation on NCLP system stability

To determine influence of thermal variation on measurement stability, the measured displacement to a flat surface held at a nominally static position orthogonal to the NCLP measurement beam, was logged over a period of several hours during variation in environmental temperature. Environmental control consisted of laboratory air conditioning (Toshiba RAV SM562KRT-E) with temperature control set at 20 ± 1 °C. The NCLP scanning room is separate from the main laboratory area accessible via a lockable door. Temperature logging was conducted out-of-hours by one operator only, to minimise variations in ambient temperature due to movement of people; the room was locked during scanning periods to ensure NCLP isolation.

A calibrated optically flat surface (Edmunds Industrial Optics, USA) made of lithium–aluminosilicate glass with low coefficient of thermal expansion ($\alpha = 0.1 \times 10^{-6}\ ^{\circ}C^{-1}$), was used as a target surface. The target was cleaned using an acetone rinse followed by distilled water and blown dry using dry nitrogen. The surface was then arranged on the NCLP, orthogonal to the incident laser beam, with the laser displacement probe at a nominal static displacement of 6 mm above the target surface. A temperature and humidity logger (Lascar Electronics, UK) with 0.1 °C and 0.5 %RH resolution recorded environmental conditions at a rate of 0.2 Hz.

Temperature and sensor displacement were then recorded at the NCLP. Short, medium, and long scanning periods were investigated under two conditions: (a) with the NCLP uncovered (open condition) and (b) with a simple inverted box enclosure over the instrument (closed condition). The enclo-

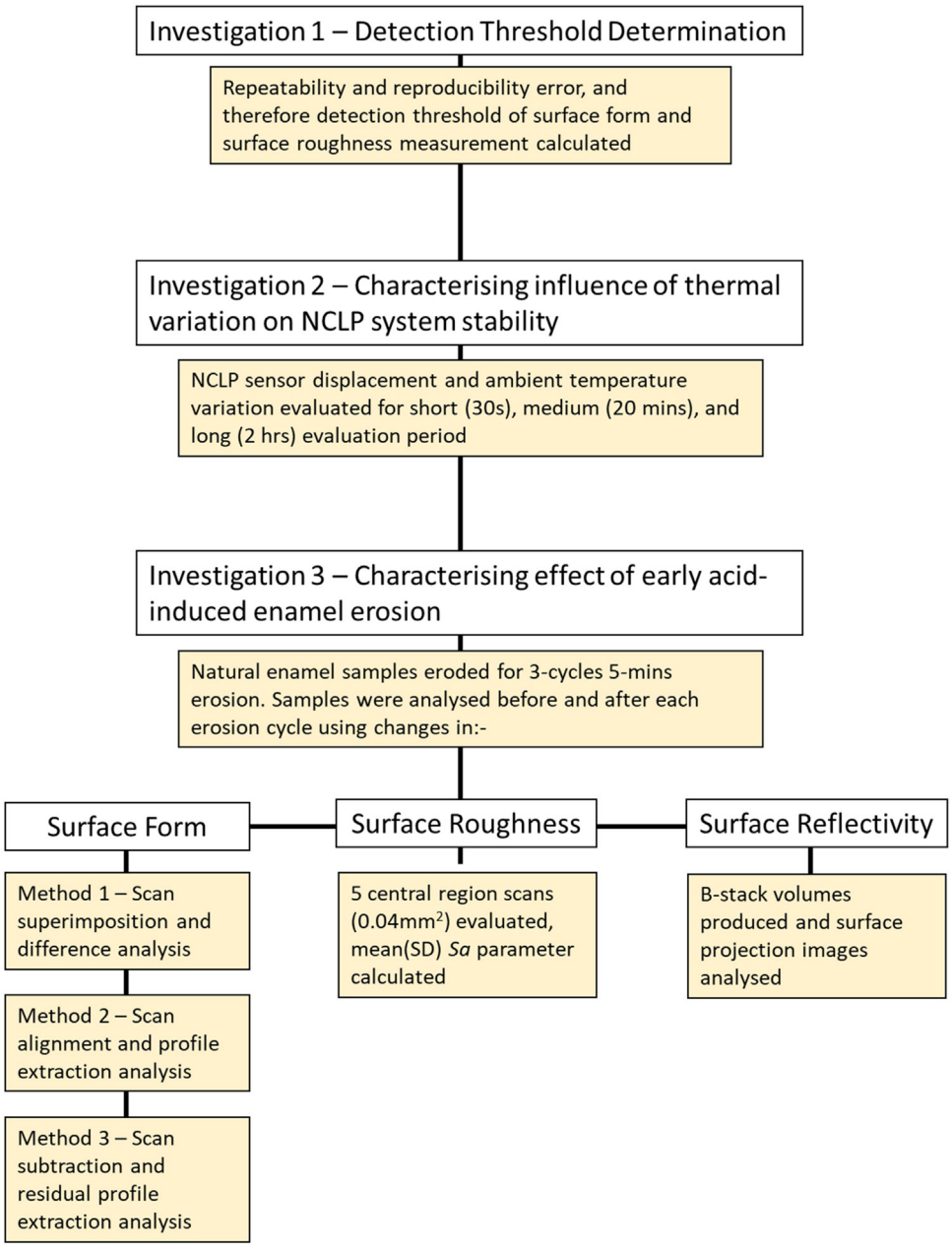

Fig. 1 – Outline of the study design.

sure provided a basic level of protection from local air currents and thus stabilises the temperature at the NCLP.

Fluctuation in scanning temperature and sensor displacement was evaluated for (1) short term stability — a 30-s evaluation period, (2) medium term stability — a 20-min period — equivalent to the time taken for a complete NCLP 3D measurement, and (3) long term stability — a 2-h evaluation. This allowed for determination of the influence of thermal effects according to the scanning time. The NCLP was programmed (Stages, Taicaan Technologies, Southampton, UK) to log the NCLP sensor displacement at 25 Hz for the short measurement and 0.8 Hz for the medium and long measurement.

The thermal variation and displacement change for each case were then evaluated for their standard deviation.

2.4. *Investigation 3—characterising effects of early acid-induced enamel erosion*

2.4.1. *Natural enamel early acid-induced erosion model*

Twelve natural enamel samples were prepared as previously described and clear polyvinyl chloride (PVC) protective barriers with a 1.5 mm diameter circular hole were placed over the maximum bulbosity of each sample. This was determined as the maximum peak detected by scanning the profile of all tooth samples prior to taping using the NCLP.

Samples were exposed to acid immersion in a repeated measures process every 5 min for three cycles, total immersion times: 5, 10, and 15 min. All samples were scanned before acid immersion to provide baseline data sets (surface form

and roughness) for comparison to after scan data. Citric acid (0.3% w/w) erosive solution was prepared, from anhydrous citric acid powder (Sigma Aldrich, Poole, Dorset UK) to deionised water, and pH adjusted to 3.2 using 0.1 M sodium hydroxide (Sigma Aldrich, Poole, Dorset UK) [17]. The titratable acidity was calculated as the volume of sodium hydroxide required to increase the solution pH to 7; this was 18.0 ml [10,17]. All samples were immersed in 10 ml of citric acid (per tooth) and agitated using an orbital shaker (62.5 RPM, Stuart mini-Orbital Shaker SSM1, Bibby Scientific, England), for 5 min before rinsing with deionised water (pH 5.8) for 2 min and left to air dry. After the PVC tape was removed, samples were replaced in the scanning jig, and surface form and roughness measurements recorded. This process was repeated to ensure measurements were obtained at 10 and 15 min erosion.

Previous unpublished pilot work attempted to use ISO 5436-1 to obtain a step height in natural enamel. However, there was no definable reference points to allow comparison between eroded and uneroded enamel. This was due to previous barrier methods proving unsuccessful in creating an isolated eroded lesion and reference enamel region [25]. Therefore, three methods for determining bulk enamel loss were proposed: scan superimposition and difference analysis; scan alignment and profile extraction analysis, and scan subtraction and residual profile extraction analysis [1,22,23]. An operator blinded to treatments conducted all analyses, and samples were randomised prior to analysis.

2.4.1.1. Surface form change measurement and characterisation.

2.4.1.1.1. Method 1—scan superimposition and difference analysis. The scan data, consisting of a Cartesian point cloud, were trimmed and transformed into a 3D surface using superimposition software (Geomagic Control 2014, Geomagic Inc, North Carolina, USA). To minimise effects of alignment error between baseline and eroded scan data sets, an initial best fit of alignment using 300 randomly selected data points was conducted before a more precise alignment using 1500 additional data points was performed. After completing superimposition, a region of interest, 0.2 mm diameter, was selected at the central region of the wear scar; this ensured minimisation of the effects of the natural topographical variation between samples. Tooth loss was then measured in μm for each erosion time point and a mean taken of all points in X, Y, and Z (automatically calculated by the software) using two outputs: mean Z-change and mean 3D total deviation between two consecutive scans.

2.4.1.1.2. Method 2—scan alignment and profile extraction analysis. All scans were loaded as a Cartesian point cloud into surface metrology software (MountainsMap, DigitalSurf, France), an offset analysis between each erosion cycle data set were initially conducted to facilitate accurate alignment and thus allowing wear scar analysis. Firstly, a 0.8 μm Gaussian filter for roughness was applied to all data sets, a spatial denoising (3 × 3) filter was applied to remove outlier points; the filtered data points were then processed together to form a composite series of images. Shift surface operator was applied which determined the offset and rotational values between the filtered roughness data in X, Y, Z. These offset values were used to correctly align all the original raw data sets according to their pre-erosion scan, further wear-scar analysis was then conducted. The post-erosion scans were subtracted from the pre-erosion baseline scan using a subtraction operator, leaving the residual data set. The palette colour was manipulated to aid visualisation of the resultant wear scar. A surface levelling operator was utilised, excluding the 1.5 mm diameter eroded wear scar region, using a linear least squares plane of best fit method. This was repeated for all post-erosion time points. Determination of change at the wear scar was expressed as residual step height, which was calculated using two quantitative outputs: resultant difference in Z (Z mean, μm), and as residual 3D step height change (μm).

2.4.1.1.3. Method 3—scan subtraction and residual profile extraction analysis. Data scans after erosion were compared with their baseline pre-eroded scans using surface metrology software (Boddies v1.92, Taicaan, Southampton, UK). Post-erosion scans were mathematically subtracted from their respective baseline scan, this produced a residual data set which was subsequently used for wear scar analysis. The residual data was levelled using best fit method excluding the central wear scar region. Differences between the uneroded region and eroded region were then quantified in microns using changes in Z-axis along a single horizontal line of reference (single mid-point step height, SPSH) [26], using 10 horizontal lines of references across the wear scar (mean single mid-point step height, mean SHC) [27], and the entire wear scar (3D step height, 3D SHC) [2].

2.4.1.2. Surface roughness change measurement and characterisation. Surface roughness was measured according to previously published protocols using surface metrology software (Boddies v1.92, Taicaan, Southampton, UK) [4,24]. A cluster of five scans each measuring 0.2 × 0.2 mm (0.04 mm^2) was selected in the central bulbosity of each natural enamel sample and scanned in a raster pattern with a 4 μm step-over distance. This was conducted using a bespoke image acquisition macro written within the motion control software (Stages™, TaiCaan Technologies, Southampton, UK) together with the assistance of a live video microscope attached to the NCLP system. This central cluster method was previously validated as representative of the natural enamel surface for measuring change in surface roughness [9].

A 25 μm Gaussian filter was applied to each scan in order to determine 3D roughness (Sa) data for each sample using metrology software (Boddies v1.92, Taicaan Technologies, Southampton, UK), and mean Sa calculated for each sample from the 5 scans according according to previously published protocols and ISO 25178 [4,24,25].

2.4.1.3. Surface reflectivity measurement and characterisation. Optical coherence tomography (OCT) was conducted, before and after each erosion cycle, using a swept-source multi-beam clinical OCT machine (VivoSight™ Michelson Diagnostics, Kent, UK) utilising a near infra-red laser (1305 nm) with optical resolution <7.5 μm. Samples were scanned in a raster pattern to produce B-stack volumes comprising 1000 B-scans of (x,z) dimension (4 × 1 mm) with y-step-over 4 μm; the resulting B-stack volumes consisted of dimension 4 × 4 × 1 mm (x,y,z). A stack analysis programme [8] extracted single full profile peak intensity average images from each B-stack volume; known

as surface projection/ reflection images. An automated macro created using ImageJ (ImageJ, Abramoff et al. [28]) was created to analyse the peak intensity (grey value) of the designated region of interest (1.5 mm diameter eroded region) before and after each erosion cycle. Peak intensity (reflectivity) analysis consisted of normalising all grey values against baseline and this was converted into a percentage; 100% reflectivity vs baseline indicated no erosion occurred at baseline. The percentage increase or decrease in normalised percentage peak intensity was determine for all erosion cycles [8,29].

2.5. *Statistical methods*

Statistical analysis was conducted using GraphPad Prism 7 (GraphPad Software Inc, California, USA). Data was assessed for normality using Komogorov–Smirnov and Shapiro–Wilks tests, and visually assessed with histograms and box plots. All the data were found to be normally distributed, and therefore mean and standard deviation was reported, between group analysis was conducted using parametric testing one-way repeated measures ANOVA with post-hoc Tukey test for multiple comparisons.

3. Results

3.1. *Investigation 1—detection threshold determination*

For the NCLP repeatability investigation, the mean (SD) surface form difference between each scan was calculated as 0.14 (0.05) μm and the NCLP repeatability was therefore calculated as 0.29 μm. Similarly, the mean (SD) surface roughness difference between each scan was 0.03 (0.01) μm and thus the NCLP repeatability for surface roughness was calculated as 0.06 μm.

However, for the NCLP reproducibility study, the mean (SD) surface form difference between each scan increased to 0.23 (0.07) μm and thus the NCLP reproducibility for surface form was calculated as 0.44 μm. For surface roughness measurements, the mean (SD) difference was 0.03 (0.02) μm and the NCLP reproducibility for surface roughness was calculated as 0.09 μm.

3.2. *Investigation 2—characterising the influence of thermal variation on NCLP system stability*

Fig. 2 and Table 1 indicate the sensor displacement variations that occur with temperature variation according to the scanning conditions of the NCLP.

During short-term evaluation, no change in scanning temperature occurred within the resolution of the temperature logger (<0.1 °C), and static stability of sensor displacement showed no significant difference between the NCLP open or closed (SD of sensor displacement 0.014 and 0.013 μm respectively). Short-term measurements were not significantly affected by thermal variation in measurement temperature, thus demonstrating the baseline repeatability of the measurement system without the influence of thermal variation in the measurement environment.

There was a cyclical temperature variation introduced by the laboratory air conditioning control (20 ± 1 °C). This produced a corresponding variation in the sensor displacement. This positive trend was evident in medium and long-term evaluations where the NCLP had no protective enclosure.

During medium-term evaluation, thermal variance (SD) of 0.260 °C was detected and corresponded with a resulting NCLP displacement SD of 0.556 μm, whilst within the enclosure NCLP thermal variance and subsequent displacement SD reduced to 0.053 °C and 0.098 μm respectively.

Similarly, during long-term evaluation, the temperature control improved (SD of 2-h temperature 0.473 °C to 0.069 °C) and the sensor displacement fluctuation dampened (1.049 μm to 0.164 μm) when the NCLP was enclosed. This relationship demonstrated a temperature sensitivity on measured displacement of the NCLP of 2218 nm/°C (2.218 μm/°C).

3.3. *Investigation 3—characterising effects of early acid-induced enamel erosion*

3.3.1. *Surface form change measurement and characterisation*

Wear scar depth as analysed using three different methods and their respective analytical outputs is shown Table 2.

3.3.1.1. Method 1—scan superimposition and difference analysis. Acid erosion caused a statistically significant increase in wear scar depth for both measurement outputs, compared to baseline, for all time points ($p < 0.0001$). Mean (SD) Z-change (μm) at 5, 10, and 15 min was 1.1 (0.9), 2.2 (1.1), 3.7 (1.6); whilst the mean (SD) total deviation (μm) for the same erosion times were 1.1 (0.8), 2.1 (1.0), and 3.5 (1.6) respectively. There was no statistically significant difference in mean Z-change and mean 3D total deviation measured for each erosion time point ($p > 0.05$). Additionally, there was no statistically significant difference in the wear scar depth calculation using either Z-mean or 3D total deviation measurement output ($p > 0.05$). Representative example of superimposition and difference analysis can be seen in Fig. 3.

3.3.1.2. Method 2—scan superimposition and profile extraction analysis. Mean (SD) Z-change (μm) after 5, 10, and 15 min erosion was 1.05 (0.59), 2.12 (1.06), 3.40 (1.75) respectively, and using mean (SD) 3D step height (μm) it was 1.49 (0.26), 2.47 (0.85), 3.71 (1.58) respectively. There was a statistically significant difference in mean 3D step height between 5 min and 15 min ($p < 0.05$). Additionally, there was no statistically significant difference in the wear scar depth calculation using either mean Z-change or mean 3D step height measurement output ($p > 0.05$).

3.3.1.3. Method 3—scan subtraction and residual profile extraction analysis. For all three measurement outputs, acid erosion after 5, 10, and 15 min caused a statistically significant increase in wear scar depth ($p < 0.0001$). Differences between each wear scar calculation method were noted and were statistically significant after 10 min erosion (mean SPSH vs mean 3D SHC, $p < 0.05$) and 15 min erosion (mean SPSH vs mean SHC, $p < 0.01$, mean SPSH vs mean 3D SHC, $p < 0.0001$). There was no

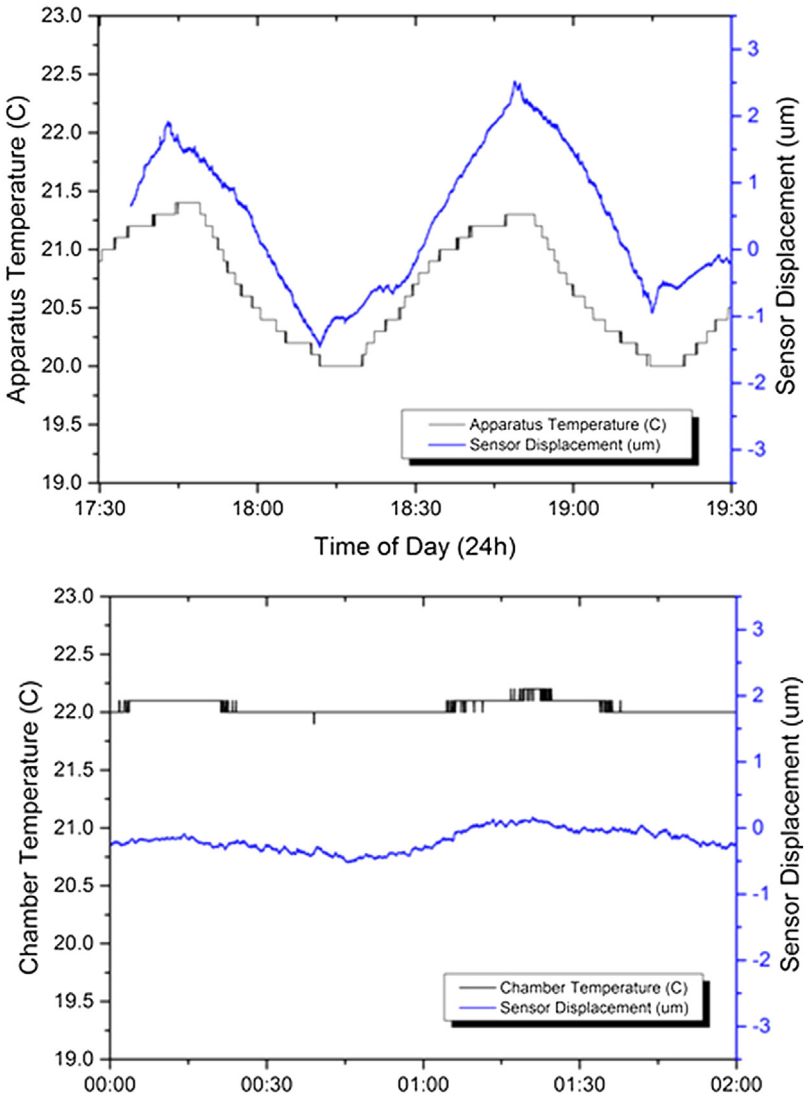

Fig. 2 – Graphs of apparatus ambient temperature and the sensor displacement without apparatus enclosure (above) and with apparatus enclosure (below). There is a clear relationship between sensor displacement and apparatus ambient temperature. The use of a thermal enclosure leads to a significant reduction in chamber and apparatus temperature which in turn minimises sensor displacement, resulting in a more stable scanning outcome.

Table 1 – Indicates the dependence of the NCLP positional accuracy on control of environmental temperature. It is apparent that a simple, low cost enclosure provides a significant improvement in thermal control and positional stability. T = 30 s indicates environmental noise floor for short term influences (non-thermal considerations). T = 20 min indicates maximum influence of thermal variance over a single NCLP 3D measurement. T = 2 h indicates maximum influence of cyclic thermal variance in the environment.

NCLP condition	Scanning evaluation period					
	30 s		20 min		2 h	
	Thermal variance [SD] (°C)	Positional variation 690 samples [SD] (μm)	Thermal variance [SD] (°C)	Positional variation 920 samples [SD] (μm)	Thermal variance [SD] (°C)	Positional variation 5500 samples [SD] (μm)
Exposed to ambient laboratory air	<0.1 (SD = 0)	0.014	0.260	0.556	0.473	1.049
Within protective enclosure	<0.1 (SD = 0)	0.013	0.053	0.098	0.069	0.164

Table 2 – Results for surface profile, surface profilometry, and peak intensity analysis are shown. For surface profile measurements, 3 methods were analysed, scan superimposition with/without profile extraction, and scan subtraction with profile extraction. Mean (SD) for each data output is determined.

	Surface profilometry										
	Scan superimposition and difference method		Scan superimposition and profile extraction method		Scan subtraction and profile extraction method			Surface roughness		Peak intensity analysis	
Erosion time (min)	Mean (SD) Z-change (μm)	Mean (SD) 3D total deviation (μm)	Mean (SD) Z-change (μm)	Mean (SD) 3D step height (μm)	Mean (SD) SPSH (μm)	Mean (SD) SHC (μm)	Mean (SD) 3D SHC (μm)	Mean (SD) surface roughness (Sa, μm)	Percentage change vs baseline (%)	Mean (SD) reflectivity (grey value)	Percentage reflection vs baseline (%)
0 (baseline)	0	0	0	0	0	0	0	1.13 (0.13)	0	48831.7	100.0
5	1.10 (0.9)	1.10 (0.8)	1.05 (0.59)	1.49 (0.26)	1.61 (1.09)	1.61 (0.56)	0.72 (0.25)	1.52 (0.23)	38.4	40026.1	82.0
10	2.20 (1.1)	2.10 (1.0)	2.12 (1.06)	2.47 (0.85)	3.06 (1.75)	2.86 (1.09)	1.72 (0.65)	1.44 (0.19)	30.3	37951.8	77.7
15	3.70 (1.6)	3.50 (1.6)	3.40 (1.75)	3.71 (1.58)	7.06 (1.26)	6.01 (1.12)	4.47 (1.25)	1.43 (0.21)	30.0	35738.8	73.2

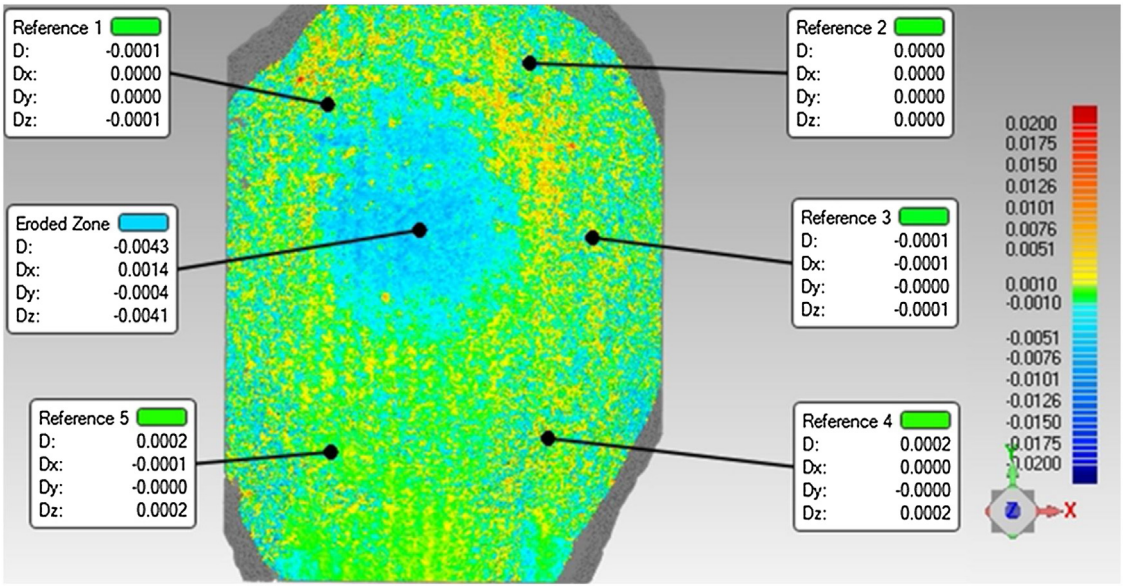

Fig. 3 – Representative example of a sample with its associated wear scar using superimposition, in blue, green denotes no change, whilst yellow denotes gain post erosion. Wear scar depth is depicted by 3D total deviation (D) and Z-deviation (Dz). The central eroded region and 5 reference regions have been analysed for allow for erosion vs non-eroded comparison (For interpretation of the references to colour in this figure legend, the reader is referred to the web version of this article).

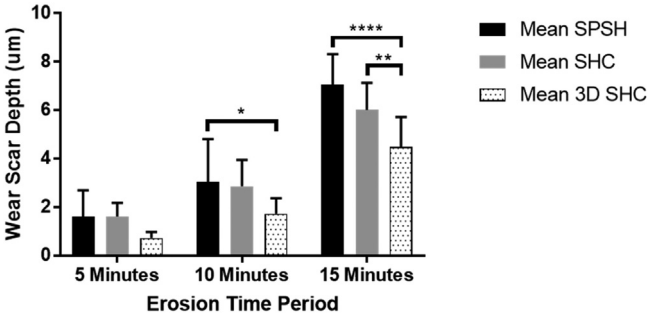

Fig. 4 – Differences between the three wear scar depth measurements were compared for the scan subtraction and profile extraction methodology. Statistical significance is denoted by * ($p < 0.05$), ** ($p < 0.01$), * ($p < 0.005$), and ****($p < 0.0001$).**

statistically significant difference in the wear scar calculation after 5 min erosion ($p > 0.05$); as seen in Fig. 4.

3.3.2. *Surface roughness change measurement and characterisation*

The mean (SD) surface roughness values for all natural enamel samples after 0, 5, 10, and 15 min acid immersion were, 1.13 (0.13) μm, 1.52 (0.23) μm, 1.44 (0.19) μm, and 1.43 (0.21) μm respectively (Table 2 and Fig. 5) and were statistically significant at all citric acid immersion time points compared to before erosion (baseline) ($p < 0.0001$). Intergroup analysis revealed statistically significant differences in mean surface roughness between 5 min and all other erosion time points (vs 10 min $p < 0.05$, and vs 15 min, $p < 0.0001$), however there was no statistically significant difference between 10 min and 15 min erosion ($p > 0.05$).

3.3.3. *Surface reflectivity measurement and characterisation*

Analysis of sample surface reflectivity, using OCT, before and after all acid erosion periods can be seen in Table 2.

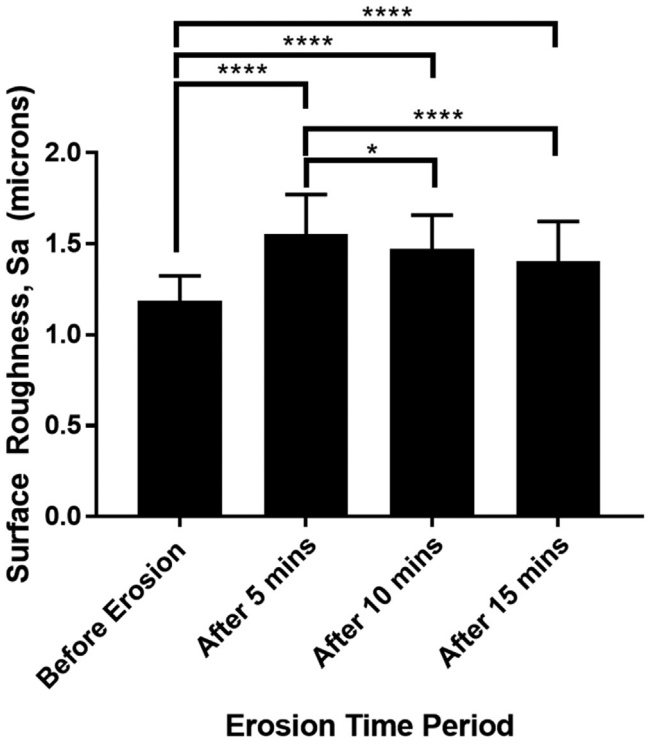

Fig. 5 – Change in surface roughness of the wear scar were determined for each erosion time point and compared to before erosion. Statistical significance is denoted by * ($p < 0.05$), ** ($p < 0.01$), * ($p < 0.005$), and ****($p < 0.0001$).**

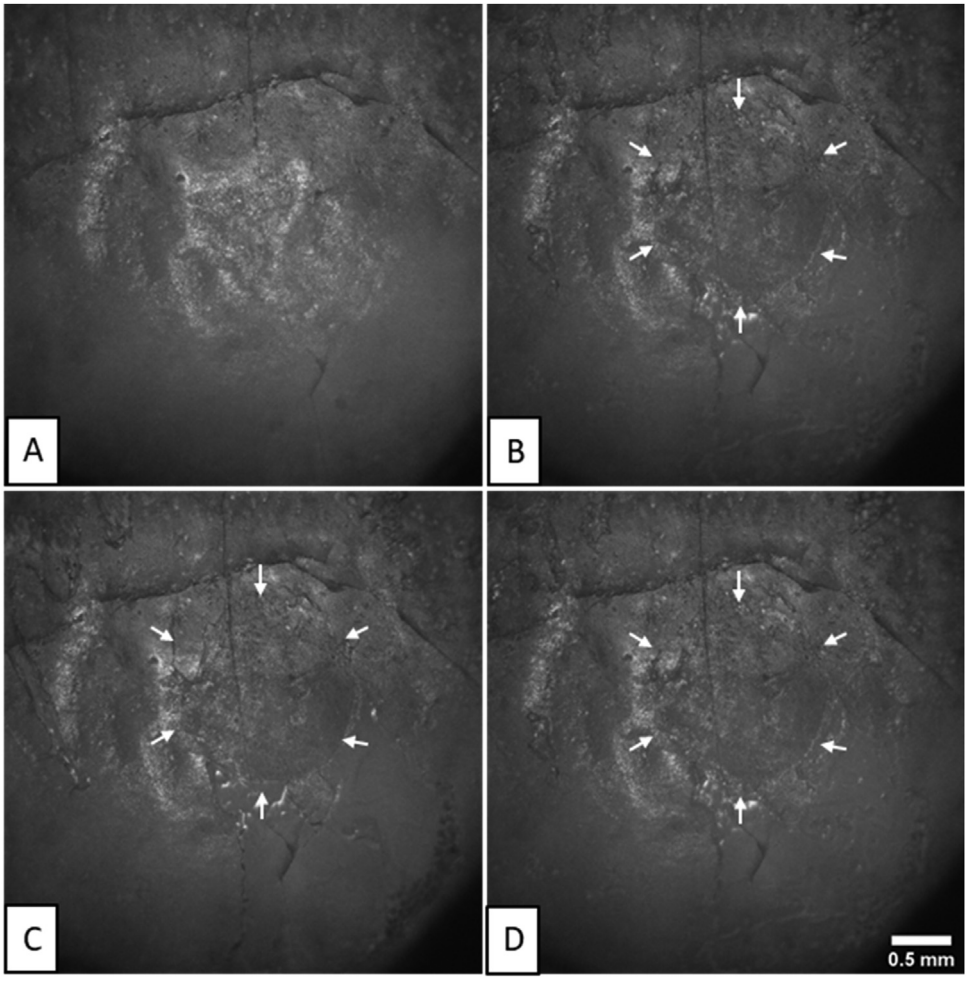

Fig. 6 – Representative example of surface reflection/projection images produced with OCT. Eroded lesion is indicated by the white arrows, and erosion times are (A) baseline, (B) 5 min, (C) 10 min, (D) 15 min erosion. Scale bar for all images in 0.5 mm.

Differences in surface reflectivity occurred after all erosion timepoints compared with before erosion. Percentage peak intensity change after 5, 10, and 15 min erosion were 82%, 77.7%, and 73.2% respectively, and were statistically significant ($p < 0.0001$) for all erosion groups compared with before erosion. However, there were no statistically significant differences in percentage peak intensity change between erosion timepoints ($p > 0.05$). An example of the surface reflectivity images can be seen in Fig. 6.

4. Discussion

The accuracy and measurement uncertainty of chromatic confocal profilometry for surface roughness measurement of polished and natural enamel surfaces has been previously studied [4], however, to the authors' knowledge, this study is the first to determine detectable threshold of monochromatic NCLP for surface form and surface roughness measurements using natural human enamel. A significant challenge in using natural enamel surfaces for both early and late erosion *in vitro* models is defining an effective barrier protocol to produce an exposed area of enamel with corresponding areas of protected/uneroded enamel to serve as reference for comparison after erosion. This is relatively easy to achieve for polished enamel samples and is one reason why *in vitro* research studying dental erosion has primarily used polished enamel surfaces [30]. However, this study is the first to utilise a novel barrier technique to provide isolation and thus creation of an eroded enamel region for comparison to region of uneroded natural enamel. This is this first study utilising a circumferential barrier creation method using adhesive tape to create dental erosion lesions on natural enamel. Surgical biopsy punch of 1.5 mm diameter provided a reliable method to reproducibly create a hole with mean (SD) 1.49 (0.03) mm. The exposed region of enamel represented the bulbosity of the natural enamel sample, this region was utilised as this would be the first region under erosive attack in the oral cavity [31]. Previously reported barrier methods utilised on polished enamel include use of adhesive tape strips [4,8,11], or nail varnish [32,33] to leave a rectangular (or similar shaped) strip of exposed enamel for erosion. In unpublished pilot work by the same authors, these barrier methods could not be successfully utilised on natural enamel to produce dental erosion lesions; adhesive tapes detached almost immediately when immersed in citric acid, and nail

varnish removal damaged the delicate eroded enamel surface.

The influence of scanning environment thermal variation on NCLP sensor displacement has not been previously studied, and for medium and long-term scanning periods it appears to have a significant influence on NCLP displacement. This will have a major impact for studies attempting to evaluate the very earliest changes that occur during acid-mediated erosion of polished and natural enamel. The effect of sensor displacement varied according to the scanning time investigated. A previous study by Holme et al. [22] indicated, but did not further evaluate, that for their scanning set up using white light interferometry (WSI), a 1 K change in temperature would result in a y-direction shift of 6.5 μm between the lens and the sample. Furthermore, no further analysis regarding how thermal variation during WSI scanning was conducted to determine its effects on subsequent scanning and step height determination. Within our study, however, we have demonstrated the effect of changing ambient temperature on NCLP sensor displacement for three different scanning time periods (short, medium, long) to reflect the different scanning durations that may occur according to the scanning parameters required to scan an object using NCLP. By doing this, our study has shown that using a scanning enclosure to stabilise ambient scanning conditions led to an improvement in NCLP sensor stability and in turn improved its measurement accuracy. Future studies utilising NCLP should therefore consider the use of a scanning enclosure to improve accuracy of subsequent measurements.

An optical flat was utilised, rather than a natural tooth sample, to determine sensor displacement, because the crystalline structure of the optical flat material will neither change size nor shape with increasing thermal changes. Therefore, a true indication of sensor displacement changes with thermal variation could be determined. Our study demonstrated a linear relationship in the region measured between sensor/apparatus temperature variation and NCLP sensor displacement. Temperature variation induced NCLP sensor displacement did not affect measurements conducted over a short scanning period (30 s). However, over medium (20 min) and long (2 h) scanning periods NCLP sensor displacement was calculated at 0.556 μm and 1.049 μm respectively. The profilometric scans conducted in this study to determine wear scar depth formation were conducted over 21 min using an NCLP system not covered nor protected from ambient thermal changes. By characterising the influence of thermal variation on subsequent sensor displacement, it was possible to account for this error in any NCLP scans being conducted over medium and long scanning periods. All studies that seek to determine the earliest effects of acid-erosion on enamel should ideally ensure ambient/sensor temperature variations are conducted in an enclosed environment, and controlled within 2 °C [34] to ensure minimisation of sensor displacement over medium-long term scanning periods.

Measuring surface form change has presented a significant challenge in erosion research due to the complex freeform nature of natural enamel and measurement errors associated with utilising NCLP [4,6,13,14]. Step height change calculation, ISO 5436-1, using post erosion scan data is considered the gold standard for determining erosive tooth wear *in vitro* for flat polished samples [30,35]. This method cannot be utilised for natural enamel samples as conventional form removal techniques and wear scar isolation — using strips of tape or other physical barriers — is not possible on freeform organic surfaces.

However, this can be determined by using either scan superimposition and comparing differences in the Z-height or by profile subtraction of before and after profile scan data and utilising the difference profile for analysis.

The utilisation of a difference profile or difference image produced by profile subtraction of before/after erosion scan data sets has been previously utilised to successfully determine bulk enamel loss in polished human enamel samples [22]. In this study by Holme et al. [22], they conducted an *in vitro* stepwise etch study using hydrochloric acid, and utilised dental amalgam as the reference region for comparison to the eroded enamel region. By subtracting the after erosion profile from the before erosion profile, the resulting difference profile was then utilised for subsequent analysis of bulk enamel loss [22]. In our study, calculation of bulk enamel loss, from the difference profile producing using profile subtraction, on natural human enamel samples as successfully demonstrated. Additionally by utilising a novel barrier technique, using PVC tape to allow for the creation of a central window of exposed enamel surrounded by region of uneroded/protected enamel, this tallowed for a direct comparison between eroded and non-eroded enamel without the use of any adjunctive dental materials as points of reference. Moreover, by utilising a bespoke scanning jig sample alignment before and after erosion was ensured to facilitate accurate superimposition or alignment of before and after erosion data sets, which therefore allowed determination of wear scar depth by profile comparison or subtraction and analysis of the difference profile.

Profile superimposition allowed for determination of changes in Z-height, either as mean Z-change or mean 3D deviation, similar to results obtained by Rodriguez et al. [1,2] who also demonstrated dimensional change using superimposition software [1,2]. Our study, however, is the first to demonstrate step height calculation using profile subtraction and either mean single point step height (mean SPSHC), mean step height (mean SHC), or mean 3D step height (mean 3D SHC). This study found no statistically significant difference ($p < 0.05$) in either measurement for the shortest erosion exposure studied (5 min). However, there was a statistically significant difference after 10 min (mean SPSH vs mean 3D SHC, $p < 0.05$) and 15 min erosion (mean SPSH vs mean SHC, $p < 0.01$, mean SPSH vs mean 3D SHC, $p < 0.0001$). Mean 3D SHC provided the lowest number for wear depth and may indicate a truer representation of wear scar depth as this is calculated from all available profiles in the wear scar. This is in agreement with previous studies which have utilised 3D SHC to determine step height change in polished [2,36] and natural enamel samples [1,2].

Previous literature has reported characterisable changes to polished enamel surfaces at 30 s erosion using surface roughness [11], 30 min using OCT [37], and 15 min using TSM [9]; however seldom have the characterisable changes to natural enamel surfaces been considered. Mullan et al. [9] demonstrated the differences in the changes in surface roughness in natural enamel samples compared with

polished enamel samples; polished samples became significantly rougher (increasing Sa values) with increased erosion compared with natural enamel samples which became significantly smoother (decreasing Sa values) after prolonged citric acid exposure times [9].

However, the results of this study indicate that during the early erosion period (5 min) surface roughness increased significantly from baseline Sa of 1.13 (0.13), up to 1.52 (0.23) μm ($p < 0.0001$), and then decreased after 10 and 15 min. Suggesting the early erosive process in natural enamel is much slower than in polished enamel samples, and the use of surface roughness can allow for determination of early changes to the surface layer of natural enamel during early erosion.

TSM demonstrated qualitative changes occurring at the amorphous surface layer and provided clear evidence at the eroded/uneroded enamel boundary which was protected by the taping isolation method. This work is supported by Mullan et al. [4] who also demonstrated surface changes to natural enamel samples after acid erosion using TSM, however, they utilised longer erosion time periods and orange juice as their erosive medium [4].

OCT provided an evaluation of the effect of early citric acid erosion on surface reflectivity. The eroded zone demonstrated reduced percentage surface reflection compared with uneroded regions as erosion time increased. This indicated that the optical properties of the amorphous surface layer were adversely affected by acid erosion. This is supported by previous *in vitro* study utilising natural human incisors embedded in resin, OCT was able to detect changes to the enamel surface following 5 and 10 min of acid erosion and detectable changes were significant after 50 and 60 min erosion [38]. Whilst, an *in-vivo* study demonstrated increase in backscattering of the OCT signal intensity as acid erosion increased, which occurred due to surface and subsurface demineralisation which was calculated up to a depth of 33 μm after 60 min erosion [39]. However, this study required 60 min of orange juice mediated acid erosion to produce a detectable effect [37–39].

This *in vitro* study has demonstrated the formation of the early erosive lesion in natural enamel, and many different methodological challenges have been overcome relating to sample isolation, and lesion characterisation. Natural enamel samples can be considered for use in *in vitro* studies to investigate the formation and progression of early acid erosion, as well as the assessment of enamel lesion remineralisation.

Whilst this was beyond the scope of this study, future work is necessary to determine the variability in physicochemical composition of natural enamel samples (due to the difference in tooth source, exposure to saliva, fluoride etc) and ascertain its impact on the dental erosion process.

5. Conclusions

NCLP detection threshold for measuring changes in surface form and surface roughness was determined for natural human enamel. Thermal variation during scanning resulted in NCLP sensor displacement over medium (20 min) and long (2 h) scanning periods, therefore this should be characterised, and its effects minimised when scanning natural enamel samples. A scanning enclosure can significantly enhance NCLP measurement stability and thus measurement accuracy. Acid-induced dental erosion wear scars in natural human enamel could be characterised using surface profilometry, surface roughness, OCT, and TSM; step height could be calculated using profile superimposition and profile subtraction techniques.

Acknowledgements

This project was supported by a Research Studentship from Unilever Oral Care, UK. The funding source had no involvement in the collection, analysis or interpretation of the data. They read the manuscript prior to submission.

REFERENCES

[1] Rodriguez JM, Austin RS, Bartlett DW. A method to evaluate profilometric tooth wear measurements. Dent Mater 2012;28:245–51, http://dx.doi.org/10.1016/j.dental.2011.10.002.

[2] Rodriguez JM, Bartlett DW. A comparison of two-dimensional and three-dimensional measurements of wear in a laboratory investigation. Dent Mater 2010;26:e221–5, http://dx.doi.org/10.1016/j.dental.2010.07.001.

[3] Paepegaey A, Barker ML, Bartlett DW, Mistry M, West NX, Hellin N, et al. Measuring enamel erosion: a comparative study of contact profilometry, non-contact profilometry and confocal laser scanning microscopy. Dent Mater 2013;29:1265–72, http://dx.doi.org/10.1016/j.dental.2013.09.015.

[4] Mullan F, Bartlett D, Austin R. Measurement uncertainty associated with chromatic confocal profilometry for 3D surface texture characterisation of natural human enamel. Dent Mater 2017;33(6):e273–81, http://dx.doi.org/10.1016/j.dental.2017.04.004.

[5] Attin T, Wegehaupt FJ. Methods for assessment of dental erosion. Monogr Oral Sci 2014;25:123–42, http://dx.doi.org/10.1159/000360355.

[6] Leach R. Fundamental principles of engineering nanometrology. Oxford, UK: Elsevier Inc.; 2009.

[7] de Groot P. The meaning and measure of vertical resolution in optical surface topography measurement. Appl Sci 2017;7:54, http://dx.doi.org/10.3390/app7010054.

[8] Mylonas P, Austin R, Moazzez R, Joiner A, Bartlett D. In vitro evaluation of the early erosive lesion in polished and natural human enamel. Dent Mater 2018;34:1391–400.

[9] Mullan F, Austin RS, Parkinson CR, Hasan A, Bartlett DW. Measurement of surface roughness changes of unpolished and polished enamel following erosion. PLoS One 2017;12:0–11, http://dx.doi.org/10.1371/journal.pone.01824.

[10] Austin RS, Mullen F, Bartlett DW. Surface texture measurement for dental wear applications. Surf Topogr Metrol Prop 2015;3:23002, http://dx.doi.org/10.1088/2051-672X/3/2/023002.

[11] Austin RS, Giusca CL, Macaulay G, Moazzez R, Bartlett DW. Confocal laser scanning microscopy and area-scale analysis used to quantify enamel surface textural changes from citric acid demineralization and salivary remineralization in vitro. Dent Mater 2016;32:278–84, http://dx.doi.org/10.1016/j.dental.2015.11.016.

[12] Mullan F, Mylonas P, Parkinson C, Bartlett D, Austin R. Precision of 655nm confocal laser profilometry for 3D surface texture characterisation of natural human enamel

undergoing dietary acid mediated erosive wear. Dent Mater 2018;34:531–7.
[13] Bell S. Measurement Good Practice Guide No. 11 (Issue 2), A Beginner's Guide to Uncertainty of Measurement. Middlesex, United Kingdom: National Physical Laboratory Teddington; 2001.
[14] Yang B, Ross-Pinnock D, Muelaner J, Mullineux G. Thermal compensation for large volume metrology and structures. Int J Metrol Qual Eng 2017;8, http://dx.doi.org/10.1051/ijmqe/2017004.
[15] Zheng J, Xiao F, Qian LM, Zhou ZR. Erosion behavior of human tooth enamel in citric acid solution. Tribol Int 2009;42:1558–64, http://dx.doi.org/10.1016/j.triboint.2008.12.008.
[16] Zheng J, Xiao F, Zheng L, Qian LM, Zhou ZR. Erosion behaviors of human tooth enamel at different depth. Tribol Int 2010;43:1262–7, http://dx.doi.org/10.1016/j.triboint.2009.12.008.
[17] Berkovitz BK, Holland G, Moxham B. Oral anatomy, histology, and embryology. 6th ed. Edinburgh: Mosby/Elsevier; 2009.
[18] Zheng J, Zhou ZR. Friction and wear behavior of human teeth under various wear conditions. Tribol Int 2007;40:278–84, http://dx.doi.org/10.1016/j.triboint.2005.09.025.
[19] Young A, Tenuta LMA. Initial erosion models. Caries Res 2011;45:33–42, http://dx.doi.org/10.1159/000325943.
[20] Shellis R, Featherstone JDB, Lussi A. Understanding the chemistry of dental erosion. Erosive tooth wear from diagnosis to therapy. Monogr Oral Sci 2014;25:163–79, http://dx.doi.org/10.1159/000359943.
[21] Kumar S, Keeling A, Bartlett D, Osnes C, O'Toole S. The sensitivity of digital intraoral scanners at measuring early erosive wear. J Dent 2018;81:39–42.
[22] Holme B, Hove LH, Tveit AB. Using white light interferometry to measure etching of dental enamel. Meas J Int Meas Confed 2005;38:137–47, http://dx.doi.org/10.1016/j.measurement.2005.04.003.
[23] Stenhagen KR, Hove LH, Holme B, Taxt-Lamolle S, Tveit AB. Comparing different methods to assess erosive lesion depths and progression in vitro. Caries Res 2010;44:555–61, http://dx.doi.org/10.1159/000321536.
[24] Attin T, Becker K, Roos M, Attin R, Paqué F. Impact of storage conditions on profilometry of eroded dental hard tissue. Clin Oral Investig 2009;13:473–8, http://dx.doi.org/10.1007/s00784-009-0253-9.
[25] Mylonas P, Austin RS, Moazzez R, Joiner A, Bartlett DW. In vitro evaluation of the early erosive lesion in polished and natural human enamel. Dent Mater 2018;34:1391–400.
[26] O'Toole S, Mistry M, Mutahar M, Moazzez R, Bartlett D. Sequence of stannous and sodium fluoride solutions to prevent enamel erosion. J Dent 2015;43:1498–503, http://dx.doi.org/10.1016/j.jdent.2015.10.003.
[27] Mistry M, Zhu S, Moazzez R, Donaldson N, Bartlett DW. Effect of model variables on in vitro erosion. Caries Res 2015;49:508–14, http://dx.doi.org/10.1159/000438725.
[28] Abramoff M, Magalhaes P, Ram S. Image processing with ImageJ. Biophotonics Int 2004;11:36–42.
[29] Schneider C, Rasband W, Eliceiri K. NIH Image to ImageJ: 25 years of image analysis. Nat Methods 2012;9:671–5.
[30] Huysmans MC, Chew HP, Ellwood RP. Clinical studies of dental erosion and erosive wear. Caries Res 2011;45:60–8, http://dx.doi.org/10.1159/000325947.
[31] Shellis RP, Addy M. The interactions between attrition, abrasion and erosion in tooth wear. erosive tooth wear from diagnosis to therapy. Monogr Oral Sci 2012;25:32–45.
[32] Amaechi BT, Higham SM, Edgar WM. Use of transverse microradiography to quantify mineral loss by erosion in bovine enamel. Caries Res 1998;32:351–6, http://dx.doi.org/10.1159/000016471.
[33] Ganss C, Lussi A, Klimek J. Comparison of calcium/phosphorus analysis, longitudinal microradiography and profilometry for the quantitative assessment of erosive demineralisation. Caries Res 2005;39:178–84, http://dx.doi.org/10.1159/000084795.
[34] ISA-TR52.00.01. Recommended Environments for Standards Laboratories. North Carolina, United States of America: The Instrumentation, Systems, and Automation Society; 2006.
[35] Lussi A, Ganss C. Erosive tooth wear: from diagnosis to therapy. 2nd ed. Switzerland: S. Karger AG; 2014.
[36] Sar Sancakli H, Austin R, Al-Saqabi F, Moazzez R, Bartlett D. The influence of varnish and high fluoride on erosion and abrasion in a laboratory investigation. Aust Dent J 2015;60:38–42, http://dx.doi.org/10.1111/adj.12271.
[37] Aden A, Anderson P, Burnett G, Lynch R, Tomlins P. Longitudinal correlation of 3D OCT to detect early stage erosion in bovine enamel. Biomed Opt Express 2017;8:1092–3.
[38] Chew HP, Zakian CM, Pretty IA, Ellwood RP. Measuring initial enamel erosion with quantitative light-induced fluorescence and optical coherence tomography: An in vitro validation study. Caries Res 2014;48:254–62, http://dx.doi.org/10.1159/000354411.
[39] Austin R, Taha M, Festy F, Cook R, Andiappan M, Gomez J, et al. Quantitative swept-course optical coherence tomography of early enamel erosion in vivo. Caries Res 2017;51(4):410–8, http://dx.doi.org/10.1159/000477098. Epub 2017 Jun 22.